ELSEVIER

International Journal of Mass Spectrometry 193 (1999) 45–56

International Journal of Mass Spectrometry

Ion trapping at atmospheric pressure (760 Torr) and room temperature with a high-field asymmetric waveform ion mobility spectrometer

Roger Guevremont[a,*], Randy W. Purves[b], David A. Barnett[a], Luyi Ding[c]

[a]*Institute for National Measurement Standards, National Research Council of Canada, Ottawa, Ontario K1A OR6, Canada*
[b]*Perkin-Elmer Sciex Instruments, Concord, Ontario, L4K 4V8, Canada*
[c]*Carleton University, Ottawa, Ontario K15 5B6, Canada*

Received 8 April 1999; accepted 8 July 1999

Abstract

A method for the confinement of ions at 760 Torr and room temperature is described. We have recently shown that a cylindrical-geometry high-field asymmetric waveform ion mobility spectrometer (FAIMS), which utilizes an ion separation technique based on the change in ion mobility at high electric fields, focuses ions in two dimensions. This article describes a FAIMS device in which the focusing is extended to three dimensions (i.e. ion trap). Characterization of the ion trap was carried out using a laboratory-constructed time-of-flight mass spectrometer. The half-life of a *m/z* 380 ion in the trap was determined to be 5 ms. (Int J Mass Spectrom 193 (1999) 45–56) © 1999 Elsevier Science B.V.

Keywords: Ion trap; FAIMS; Ion mobility

1. Introduction

The radio-frequency (rf) quadrupole ion trap was invented by Paul and Steinwedel in 1953 and described in the patent of the quadrupole ion filter [1]. In 1989, the Royal Swedish Academy of Sciences awarded half of the Nobel Prize in Physics [2] jointly to Paul [3], and to Dehmelt [4], for their pioneering work with the ion trap. Since then, the ion trap has been developed into commercial mass spectrometric systems, and ion traps have been reported with impressive capabilities including mass resolution exceeding 10^7 [5], mass ranges in excess of 50 000 Da [6], and up to nine consecutive collisional dissociation reactions starting with a single ion species [7]. The rf quadrupole ion trap, despite these capabilities, cannot operate at a pressure of 760 Torr because the ion motion in these devices [8,9] requires a long mean-free path, hence reduced operating pressure. Furthermore, all existing ion optical devices capable of confining, or trapping ions, including the rf quadrupole ion trap, fail to function at atmospheric pressure (760 Torr).

Ions at atmospheric pressure are routinely separated with ion mobility spectrometry (IMS) [10–12], a technique also known as plasma chromatography [11]. With IMS, the ions are gated into a flight tube consisting of several conductive rings that are held at a series of linearly varying voltages, to form a

* Corresponding author. E-mail: roger.guevremont@nrc.ca

PII S1387-3806(99)00148-7

uniform electric field along the length of the flight tube. Thus, ions are separated in the flight tube as a function of time. The ion cloud, which is drifting through the flight tube of an IMS instrument, is subject to spreading by diffusion, ion–ion repulsion, and gas turbulence. There is no known method to reduce the expansion of the ion cloud. Consequently, the resolution and sensitivity of IMS is limited by the physics, and kinetics, of these processes.

Modern mass spectrometric instrumentation is routinely used to detect ions that are formed at atmospheric pressure, via techniques including atmospheric pressure ionization (API) [13], and electrospray ionization (ESI) [14–17]. Electrospray ionization is possibly the most important method that has been developed to date for producing gas-phase ions of biochemical, and pharmaceutical interest, for introduction into a mass spectrometer.

Despite the existence of ion focusing and trapping devices suitable for operation at reduced pressures, the ions formed at 760 Torr by API and ESI sources have been transported, at atmospheric pressure, to the orifice of the mass spectrometer without the benefit of an instrumental method for ion focusing. Consequently, the ions produced by these sources will disperse in space due to a combination of divergent electric fields (ESI), gas turbulence, ion–ion repulsion, and diffusion.

The newly developed technique of high-field asymmetric waveform ion mobility spectrometry (FAIMS), has been shown to be capable of ion separation [18,19] and focusing [19,20] in two dimensions at atmospheric pressure and room temperature. In this article, we describe the extension of the ion focusing capability of FAIMS, and the development of a three-dimensional ion trap which operates at 760 Torr and room temperature.

2. Introduction to high-field asymmetric waveform ion mobility spectrometry

FAIMS is a technique that exploits the change of the mobility of an ion at high electric fields. Fig. 1 illustrates the ratio of ion mobility at high electric

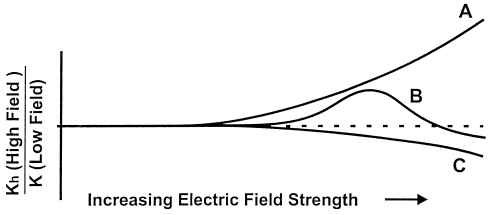

Fig. 1. Hypothetical dependence of ion mobility on electric field for three types of ions.

field, K_h, relative to the mobility at low electric field, K, for some hypothetical ions A, B, and C. For example, the ratio of K_h/K for a type A ion increases with electric field, a behavior which is typical of small ions. Several examples are discussed by Mason and McDaniel [12].

Fig. 2 illustrates the motion of an ion between two parallel plates, as used in the first version of FAIMS described by Buryakov et al. [18]. The ion is transported along the space between the plates by a gas flow (not to scale). The lower plate is at ground potential whereas the upper plate has a high voltage asymmetric waveform, $V(t)$, applied to it. A (simplified) version of the waveform consisting of a high voltage period t_{high}, and a low voltage period t_{low}, is shown at the bottom of the figure. The peak voltage of the waveform is called the dispersion voltage, DV. The waveform is synthesized with $V_{high}t_{high} + V_{low}t_{low} = 0$, where V_{high} and V_{low} are the applied voltages

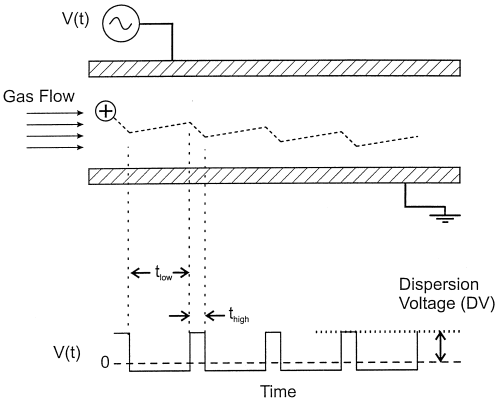

Fig. 2. Schematic of the ion motion between parallel plates during the application of an asymmetric waveform shown as $V(t)$; the ion is transported horizontally by a gas flow (distance not to scale).

during the high and low voltage periods. During the high electric field period of $V(t)$, the distance the ion travels away from the upper plate is $K_h E_{high} t_{high}$. The distance traveled toward the upper plate during the low field portion of $V(t)$ is $KE_{low}t_{low}$. Thus, the distances traveled during the low and high voltage periods of the waveform are equal if the ion mobility K_h is equal to K. If E_{high} is strong enough to cause K_h to differ from K, then the ion migrates toward one of the plates, as illustrated in Fig. 2 for a type A ion (from Fig. 1). A low voltage dc offset, called the compensation voltage, CV, can be applied to the plates to stop the net migration toward either plate. Experimentally, the value of CV is typically between −50 and +50 V when DV is 3300 V. Since the mobility of an ion at high field is dependent on (unknown) properties of the compound, only those ions with a particular ratio of K_h/K will successfully travel parallel to the plates at a given CV. FAIMS is therefore capable of ion separation.

Carnahan and Tarassov [21] designed a FAIMS system using cylindrical electrodes, rather than the plates described by Buryakov et al. [18]. The asymmetric waveform is applied to the inner of two concentric cylinders, and the annular space between the cylinders corresponds to the space between the parallel plates described by Buryakov *et al*. This FAIMS, with cylindrical geometry formed the basis of a new instrument called a Field Ion Spectrometer® (FIS®), built by Mine Safety Appliances Company, Pittsburgh, PA.

The cylindrical geometry provided considerable improvement in sensitivity over the flat plate design because an ion focusing region was formed in the annular space between the cylinders [20]. At an appropriate combination of DV and CV, an ion will travel with the gas flow along the length of the FAIMS device, but because of the focusing effect the ion will be unable to travel in either direction radially. This focusing decreases ion loss to the walls, and therefore the ion transmission through the device can be high. This high ion transmission, combined with ion separation, suggests that FAIMS is an ideal interface between an API or ESI ion source at atmospheric pressure, and a mass spectrometer. The design of an ESI system [22] and application to separation of structural isomers of amino acids (leucine and isoleucine, both m/z − 130) has been demonstrated [23].

A consequence of the ion focusing phenomenon in FAIMS is a significant change in the motion of an ion when the waveform voltage polarity is reversed. If $V(t)$ is inverted, the trajectory of an ion, which was focused in the FAIMS analyzer, will become unstable, and the ion will be lost from the analyzer. As a simplification, upon application of the mirror image of $V(t)$, the fields in the FAIMS analyzer also are mirrored, and the focusing fields are replaced by defocusing fields. Thus, the application of the two waveforms are considered separately, as mode 1 and mode 2. When considering positive ions, these are abbreviated to mode P1 and P2, and similarly, modes N1 and N2 refer to negative ions [22]. In general, an ion whose mobility increases with electric field appears in spectra in modes P1. Usually these ions have m/z below about 300. These are only guidelines, because (1) there are exceptions, and (2) an ion can (in principle) be detected in both modes [22].

3. Theory: ion trajectory calculations for the FAIMS ion trap

The physics of the two-dimensional focusing of ions in FAIMS was considered previously [20]. In this article, the ion trajectory calculations, which show the ion behavior in the three-dimensional FAIMS ion trap, will be described and the experimental verification of this phenomenon will follow.

The trajectories of ions moving within the FAIMS ion trap was calculated in two phases. The first phase established the electric fields within a cylindrical structure containing three electrodes, the inner and outer FAIMS cylinders, and a sampler cone, shown in Fig. 3(a). This electric field calculation was performed using the “relaxation” technique often used in fluid dynamics [24]. The second phase was the calculation of ion trajectories by breaking down the ion motion into a series of small translational steps based on the local electric fields due to the asymmetric waveform, and the dc voltages on the electrodes and the sampler

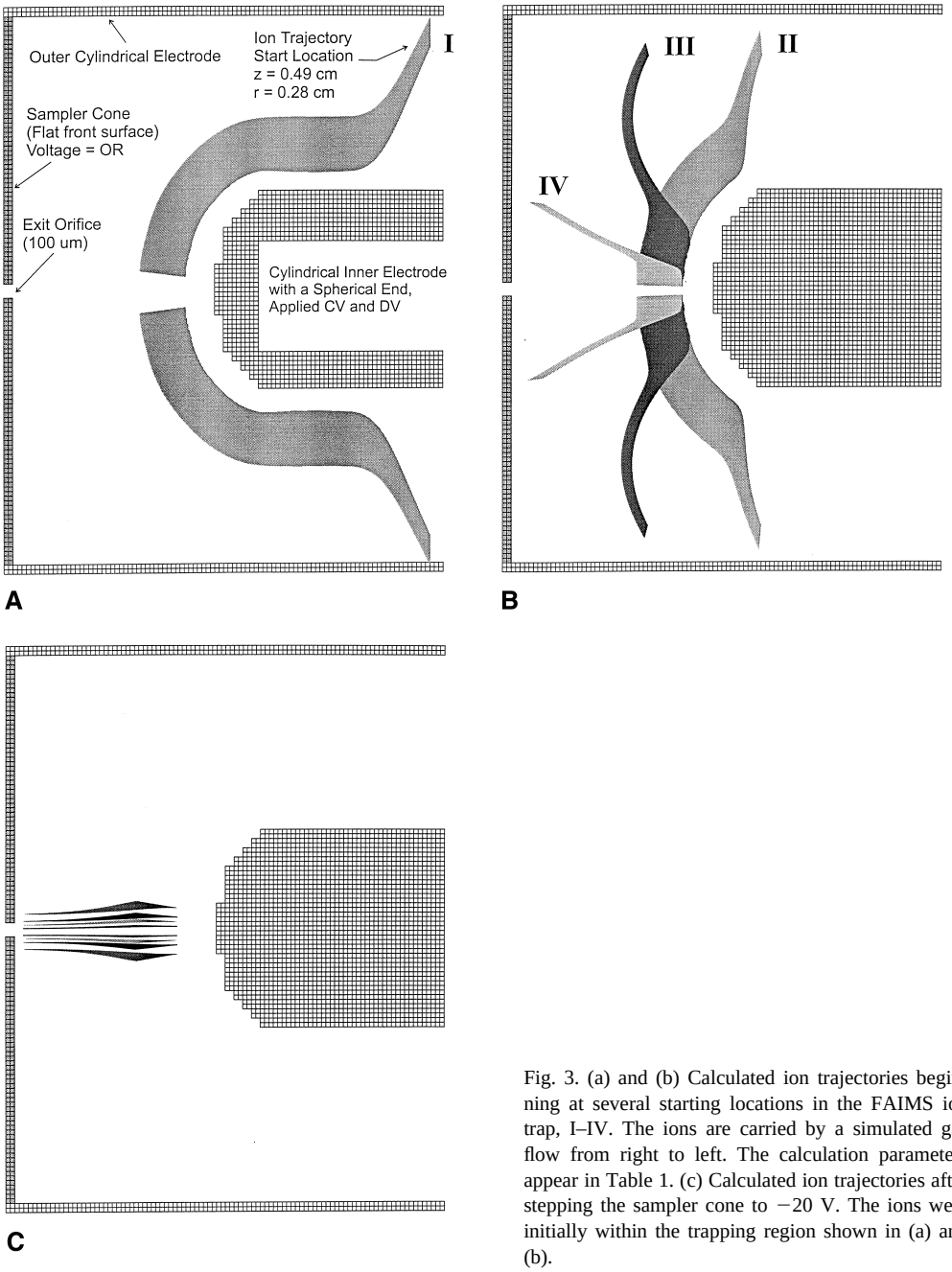

Fig. 3. (a) and (b) Calculated ion trajectories beginning at several starting locations in the FAIMS ion trap, I–IV. The ions are carried by a simulated gas flow from right to left. The calculation parameters appear in Table 1. (c) Calculated ion trajectories after stepping the sampler cone to −20 V. The ions were initially within the trapping region shown in (a) and (b).

cone. The details of the parameters used for this calculation appear in Table 1. Fig. 3(a) and (b) include calculated ion trajectories starting at four different locations (i.e. locations marked I–IV) with the outer cylindrical electrode, and the sampler cone (OR, orifice voltage) both held at ground potential. For the calculations described here, a gas flow was simulated as a constant translation of the ion from right to left in the figures, and did not include turbulence or changes in gas velocity near surfaces. In addition, the trajec-

Table 1
Parameters used in ion trajectory calculations[a]

Scale	200 points/cm
Axial, number of points	100 points
Radial, number of points	62 points
Inner electrode, o.d.	2.0 mm
Outer electrode, i.d.	6.0 mm
FAIMS analyzer region width	2.0 mm
Inner-sampler distance	2.2 mm
Starting location (radial)	*r* varied
Starting location (axial)	*z* varied
DV	2500 V
CV	−19 V
Outer electrode offset	0 V
Sampler cone (storage)	0 V
Sampler cone (extraction)	−20 V
Waveform frequency	200 kHz
Waveform, square	2:1 high/low voltage
Calculation: steps/waveform	200 steps
Applied axial velocity	−50 cm/s

[a] Assumed ion mobility at high field (K_h) for trajectory calculations: $K_h = 2.3\ (1 + 1.1 \times 10^{-7}\ E + 1.29 \times 10^{-10}\ E^2)$, where E is the field at 760 Torr (V/cm).

tory calculations did not include the effects of space–charge or ion–ion repulsion.

The motion of the ions in FAIMS, shown in Fig. 3(a) and (b), can be described as the superposition of several independent motions. First, the ion oscillates back and forth along a direction approximately perpendicular to the nearest surface of the inner electrode due to the ~200 kHz asymmetric waveform. These oscillations are "blurred" into what appears to be a wide "band" in Fig. 3. Second, the ion falls into the two-dimensional trapping region along the length of the inner electrode. Finally, the ion is carried along the electrode by the "synthetic" application of translation representing the flow of gas. The calculation of the ion trajectory was continued until the final location of the ion was unambiguous. In all examples, the ion traveled to the spherical terminus of the FAIMS inner electrode, and was unable to proceed further, even with the flow of gas. As shown in Fig. 3(a) and (b), the final location of the ion was independent of the starting location.

Fig. 3(c) illustrates the motion of ions from near the trapping region when the voltage of the sampler cone (OR, orifice voltage) is decreased stepwise from 0 to −20 V. The ions, which were captured in the trap when using the conditions shown for Fig. 3(a) and (b), are extracted from the trap and travel toward the sampler cone as shown in Fig. 3(c). A 100 μm orifice leading into the vacuum of a mass spectrometer is located at the center of the sampler cone.

4. Instrumentation

4.1. FAIMS–TOFMS

The experimental setup for the time-of-flight mass spectrometric evaluation of the FAIMS ion trap is shown in Fig. 4(a). The FAIMS ion trap operates at atmospheric pressure and is located to the left of the sampler cone in Fig. 4(a). The vacuum components of the low resolution, linear time-of-flight mass spectrometer (TOFMS) are shown to the right of the sampler cone in Fig. 4(a). These components include a differentially pumped interface, an octopole ion guide, ion acceleration grids, and an electron multiplier detector. Typical operating parameters for the system are reported in Table 2. The timing diagram for control of the FAIMS offset voltage (V_{FAIMS}), DV, CV, sampler cone voltage (OR), and the TOFMS acceleration pulse appear in Fig. 4(b).

The FAIMS ion trap is composed of two concentric cylinders shown in cross section. The outer electrode is approximately 7 cm in length, has a 0.6 cm inner diameter, and is mounted 0.5 mm from the front surface of a sampler cone. The inner electrode has a 0.2 cm outer diameter, terminating in a spherical surface about 0.3 cm from the sampler cone. The inner electrode is held within the outer electrode by an insulating Torlon (DSM Engineering Plastic Products Inc., Reading, PA, USA) spacer. A port in the outer electrode permits entry of a carrier gas (C_{in}) at about 1.2 L/min. This carrier gas flows along the annular space between the outer and inner electrodes (FAIMS analyzer region), and exits through three vents which include: the gap between the outer electrode and the sampler cone, the ion inlet port (I_{in}) communicating with the ionization chamber, and the 100 μm orifice in the sampler cone. The portion of C_{in} which flows out through I_{in} serves as a "curtain gas" flow to ensure

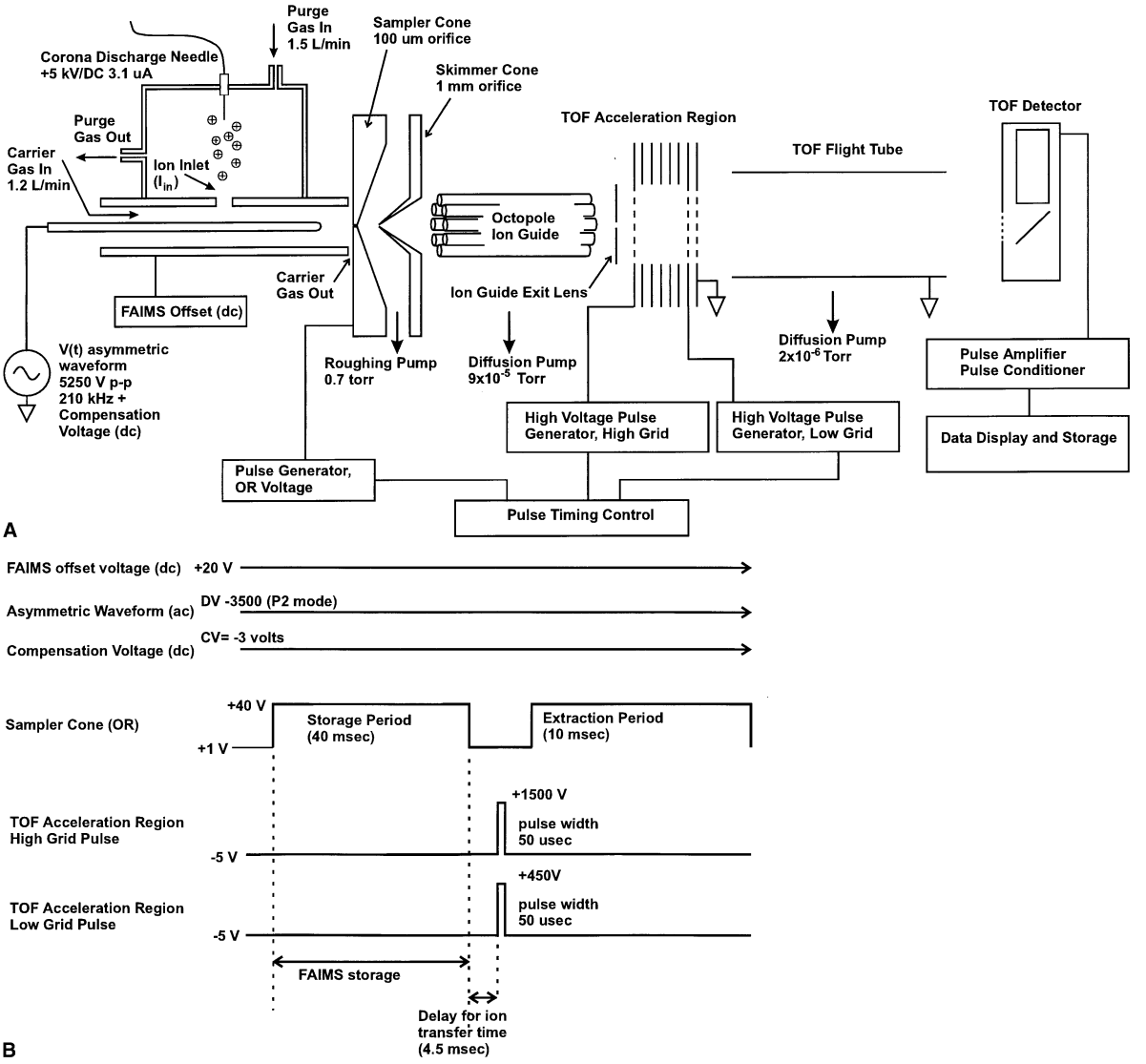

Fig. 4. (a) Schematic of the combined atmospheric pressure FAIMS ion trap, and a linear time-of-flight mass spectrometer (TOFMS). (b) Timing diagram of the electronics of the FAIMS–TOFMS system.

that the gas flowing along the FAIMS analyzer region is free of impurities.

A corona discharge needle is supported about 1 cm from I_{in}, within an ionization chamber that is about 4 cm in diameter. The ionization chamber is flushed with purified gas (purge gas in, P_{in}). This gas, combined with the carrier gas that enters the chamber through I_{in}, exits through a purge gas out (P_{out}) port.

The FAIMS ion trap is operated with three electrical power sources. First, the asymmetric waveform and CV are both applied to the inner electrode. Second, the FAIMS is held at a dc offset voltage (V_{FAIMS}), allowing a voltage difference to be established between the FAIMS unit and the sampler cone. Finally, a pulsed power supply is used to set the sampler cone voltage (OR) in two possible states; one for storage of ions, and the second for extraction of ions from FAIMS. In a typical experiment, the OR is

Table 2
Summary of typical instrumental operating conditions of FAIMS-TOFMS for ion trapping experiments

FAIMS conditions	
Ionization method	corona discharge
Discharge voltage	+5 kV
Discharge current	3.1 μA
Inner electrode radius	1 mm
Outer electrode radius	3 mm
FAIMS dc offset: V_{FAIMS}	+20 V
Inner electrode dc	+17 V
Compensation voltage (CV):	−3 V
Dispersion voltage (DV)	−3500 V (P2 mode)
Asymmetric waveform frequency	210 kHz
Asymmetric waveform	$\frac{2}{3}$ DV sin (θ) + $\frac{1}{3}$ DV sin (2θ − π/2)
Bath gas	nitrogen, purified
Bath gas pressure	770 Torr (approx)
Sample compounds	trace impurities
Carrier gas in	1.2 L/min
Purge gas in	1.5 L/min
Interface conditions	
Sampler cone (OR)	pulsed
Sampler cone (OR) high	+40 V
Sampler cone (OR) low	+1 V
Time OR high	30 ms
Time OR low	10 ms
Skimmer cone	0 V
Interface vacuum	0.7 Torr
Octopole ion guide conditions	
Frequency	1.2 MHz
Voltage	±700 V
Octopole DC offset	−4 V
Octopole AC setting	200 *m/z*
Octopole exit lens	−5.5 V
Octopole vacuum chamber	9×10^{-5} Torr
TOFMS conditions	
Acceleration high grid on	+1500 V
Acceleration low grid on	+450 V
Acceleration high grid off	−5.5 V
Acceleration low grid off	−5.5 V
Acceleration pulse width	50 μs
Flight tube offset	0 V
Multiplier acceleration	−5000 V
Multiplier	−1800 V
Vacuum chamber	2×10^{-6} Torr
Flight tube length	62 cm
Acquisition average	5000 cycles
Ion peak width at 27 μs	0.2 μs
System timing	
Repeat frequency	20 Hz
Cycle time	50 ms
Time A	0 ms
Time B	40 ms
Time C	44.55 ms
Time D	44.60 ms
Sampler cone control	A–B time window
TOFMS acceleration control	C–D time window

+40 V for 30 ms during trapping of the ions and at +1 V for 10 ms during ion extraction (i.e. with V_{FAIMS} + 20 V, and CV −3 V). After the initiation of the ion extraction by lowering OR, the cloud of ions, which was located near the terminus of the inner electrode, moves towards the orifice in the sampler cone, as shown in the simulation illustrated in Fig. 3(c).

A pulse of ions from FAIMS enters the TOFMS through a differentially pumped interface, and into a custom-made octopole ion guide (ABB Extrel, Pittsburgh, PA, USA). The octopole ion guide is operated at low pressure (9×10^{-5} Torr) so that the transit time, and thus broadening of the pulse of ions inside the octopole, is minimized. The ions pass from the octopole, through an exit lens, and into the acceleration grids of the TOFMS. The acceleration region of the TOFMS is composed of 3 fine mesh metal grids (Buckbee Mears, St. Paul, MN). The grid, which is located closest to the flight tube, is held at constant ground potential. The other two grids [i.e., "high grid" and "low grid" in Fig. 4(a)] are each connected to a high voltage pulse generator (GRX-2.0K-H, Directed Energy, Inc., CO). The grids are set at low and high voltage states, controlled by external pulse generator digital logic. In the low voltage state, i.e. −5.5 V, the ions travel from the exit lens of the octopole ion guide through the grids. The grids are then rapidly stepped (less than 0.1 μs risetime) to high voltage, and held constant for about 50 μs. The acceleration region is designed so that the ions have energy (in part) dictated by their starting location between the two pulsed acceleration grids. This difference in energy gives the device a capability for "spatial" focusing, which means that all of the ions with a given *m/z*, regardless of their starting position in this region, will reach the detector simultaneously. Even with spatial focusing, the linear TOFMS has limited resolution because the ions (in this system) enter the acceleration region with a range of kinetic energies.

4.2. Operation of the FAIMS ion trap–TOFMS

The FAIMS ion trap–TOFMS includes two pulsed components, the sampler cone and the TOFMS acceleration grids. The TOFMS acceleration region was pulsed at a series of selected delay times relative to the pulse applied to the sampler cone. At each delay time, a mass spectrum, which was an average of a minimum of 2000 repeat pulse sequences, was collected. In this way a series of TOFMS spectra, which monitored the arrival time versus intensity profile of the ions relative to the application of the pulse applied to the sampler cone, were acquired. If an assembly of ions has been trapped at the spherical terminus of the FAIMS inner electrode, the pulse of ions should be characterized by the appearance of a strong, transient signal, at some delay time after the sampler cone was stepped to a low voltage. This signal would then decay to a constant value that would be detected if the sampler cone was held at the low voltage (e.g. +1 V) state continuously. The trapping phenomenon was further investigated by varying the time during which the sampler cone was held in the high voltage state, thus varying the "trapping time." The number of ions trapped should be a combination of an input flux of ions (constant), and an ion loss mechanism wherein (for example) the rate of loss is proportional to the density of ions in the FAIMS ion trap. This kinetic evaluation of the ion storage in FAIMS is described in Sec. 5.4.

5. Results and discussion

5.1. TOFMS and compensation voltage spectra

Several preliminary experiments were conducted to establish practical conditions that would demonstrate ion trapping with FAIMS. Protonated water cluster ions are easily detected when using a corona discharge ionization source. However, these ions are at very high density, and therefore would be expected to either fill the ion trap too rapidly, or have lifetimes too short for the present study. Therefore, higher mass ions observed in P2 mode [19] were investigated. The abundance of the high mass ions was low since they were formed from trace impurities in the carrier gas. As previously reported [19], P2 mode is much less susceptible to contaminants than P1 mode, and the lifetimes of these ions are expected to be maximized

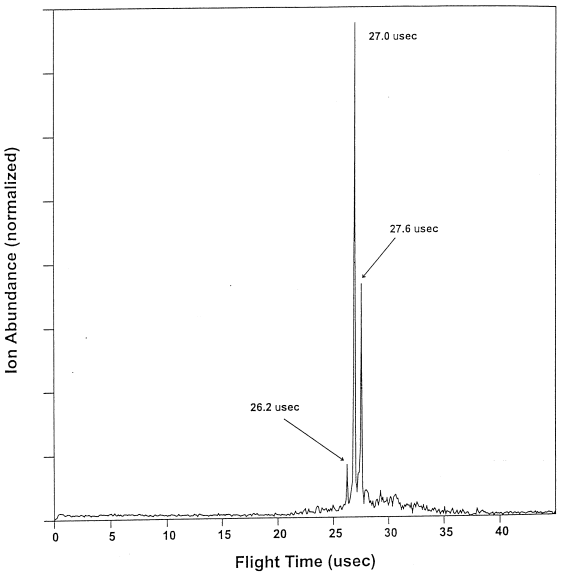

Fig. 5. Typical TOFMS spectrum of the ions used to evaluate the FAIMS ion trap (DV −3500 V, CV −3 V, P2 mode).

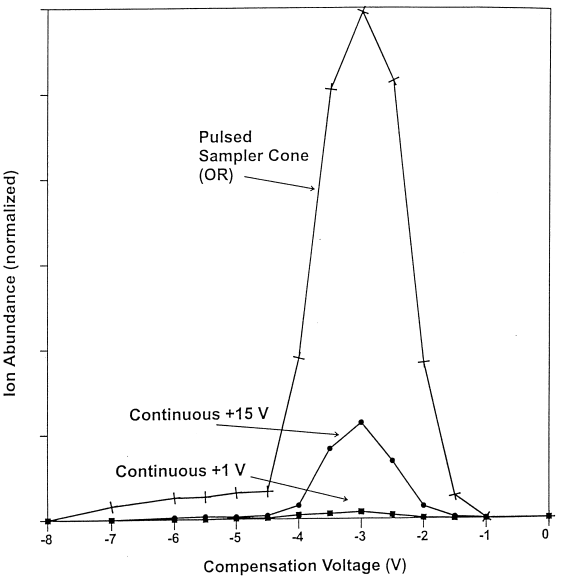

Fig. 6. Compensation voltage spectra of the *m/z* 380 ion. Repeat CV scans were collected using OR pulsed, or held constant at +15 or +1 V.

since loss to the walls of the FAIMS device through changes in chemical structure (e.g. changes in level of hydration) would be minimized.

Fig. 5 illustrates an example of a FAIMS–TOFMS spectrum acquired with DV −3500 V and CV −3.0 V. The mass-to-charge ratio of the trace contaminant with a flight time of 27.0 μs [*m/z* 380 ($\pm$10)] was determined using a calibration based on the flight times of some lower mass ions including the protonated water cluster ions. Several impurity ions appear in the spectrum, however only the ion of highest abundance (flight time 27.0 μs) was used in the present study.

The mass spectrum in Fig. 5 is not a conventional API spectrum. The low mass ions, including protonated water cluster ions, are conspicuously absent. The spectrum in Fig. 5 was collected in P2 mode, and the low mass ions have been filtered out by FAIMS. Moreover, recall that only those ions with approximately the correct ratio of K_h/K can be transmitted at a particular combination of DV and CV; the spectrum in Fig. 5 therefore displays a small subset of the mixture of ions delivered from the ionization chamber into the FAIMS device.

The separation of ions in FAIMS is controlled by CV [19]. The optimum CV of transmission of the *m/z* 380 ion through FAIMS at a DV of −3500 V (P2 mode) was experimentally determined, and the results shown in Fig. 6. The ion intensity at each experimental point in Fig. 6 was acquired by averaging the spectra recorded from 5000 repeat TOFMS acceleration pulses. The CV was adjusted manually, using a digital voltmeter to monitor the applied voltage. The traces appearing in Fig. 6 correspond to three methods for the collection of CV scans including: (1) pulsed OR with detection at 4.5 ms after the reduction of OR; continuous ion transport from FAIMS through to the TOFMS with (2) OR of +15 V and (3) OR of +1 V. The CV corresponding to the maximum ion transmission of the *m/z* 380 ion was comparable for these three methods of data acquisition (CV = −3 V).

5.2. Ion transport delays within the ion optics of the FAIMS–TOFMS

Fig. 7 illustrates the results of an experiment designed to determine the response time of the com-

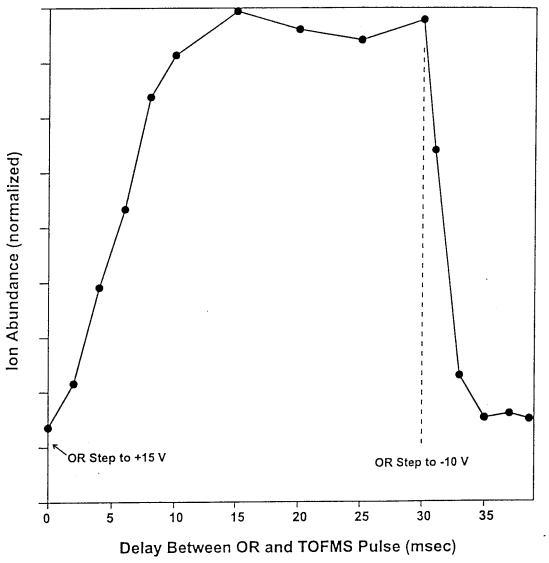

Fig. 7. Evaluation of the response time of the FAIMS–TOFMS. At $t = 0$, OR was pulsed to +15 V (start ion transmission), and at 30 ms, OR was stepped to −10 V (stop ion transmission).

bined FAIMS ion trap–TOFMS system. The OR was stepped between two values, one which was suitable for ion transmission through the FAIMS and into the vacuum system (+15 V), and a second voltage, which was unsuitable for either trapping or ion transmission (−10 V). Fig. 7 illustrates the TOFMS intensity of the *m/z* 380 ion at a series of times relative to the OR transitions of both high to low, and low to high voltages.

The "down" transition of OR occurs at 30 ms in Fig. 7. After this transition, the electric field will prevent any (positively charged) ions from passing between the sampler cone (OR = −10 V) and the skimmer cone (0 V). This down transition should create an extremely abrupt decrease in ion flux to the octopole ion guide. Experimentally, the decrease in ion density lasted about 2 ms. This delay is attributed to (1) the range of kinetic energies of the ions entering the octopole and (2) reduction in the kinetic energies of some fraction of the ions through collisions with the residual gas within the octopole. Since the octopole is an ion guide, this longitudinal spreading will be accentuated as ions, which have undergone collisions with the residual gas, will remain contained within the octopole.

The "up" voltage transition of OR from low to high voltage occurs at time 0 ms in Fig. 7, and the time required for the intensity of the TOFMS spectra to reach a plateau is about 10 ms. At the low state of OR, relatively few ions are located near the end of the inner FAIMS electrode because an electric field pulls the ions against the sampler cone (V_{FAIMS} + 20 V, OR −10 V). When OR is raised to +15 V, the relatively low density of ions which was located in front of the terminus of the inner electrode of FAIMS is augmented by newly arriving ions which have been passing along the annular region of the FAIMS cylinders. The ion density increases until ions pass to the sampler cone, and through the orifice. From the discussion of the down edge of the OR voltage pulse, it requires a minimum of 2 ms for changes in ion density to be transmitted through the octopole. The remaining 8 ms delay is attributed to the increase of ion density in the FAIMS trapping region.

5.3. Experimental verification of ion trapping in FAIMS

Fig. 8 shows the measured intensity of the ion (*m/z* 380) collected at various times after the down transition ($t = 0$) of the sampler cone. The sampler cone was pulsed from the high voltage state (OR + 40 V) which was suitable for ion trapping, to the low voltage state (OR + 1 V), thereby extracting ions from the FAIMS ion trap. The ions require about 5 ms to travel through the system to the TOFMS acceleration region. The pulse of ions is widened during passage, and appears to be about 3 ms wide (half-height) when detected. This peak delay time, and peak width is consistent with the response times determined by the experiments described in Sec. 5.2, and shown in Fig. 7. A more intense pulse of ions might be observed using a detection system with faster response.

Fig. 8 also includes two horizontal lines corresponding to collection of continuous mode data at two different settings of OR. The lower intensity data was collected with OR = +1 V, which corresponds to the low state of OR when operating in pulsed mode. The

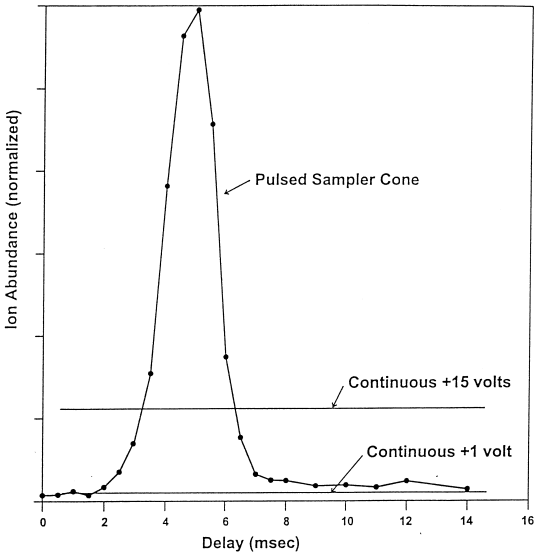

Fig. 8. TOFMS detection of the pulse of ions (*m/z* 380) after a 40 ms ion storage period in FAIMS. At $t = 0$, OR was stepped down to +1 V to extract the trapped ions into the TOFMS. The acceleration grids of the TOFMS were activated after the delay times shown. The intensity of the *m/z* 380 ion measured with constant (no trapping) OR = +1 and +15 V, is shown for comparison.

higher intensity, horizontal trace, was collected at an experimentally optimized setting of OR = +15 V. The enhanced signal intensity at OR + 15 V has been determined [25] to be the result of "focusing" of ions into the orifice of the sampler cone by the cylindrical inner electrode of FAIMS. Ion trajectory modeling has shown that the ions passing around the spherical terminus of the inner electrode will be focused towards the center channel as they pass by the end of the electrode, with a concomitant increase in sensitivity.

For the purposes of establishing the existence of a cloud of trapped ions in a region near the spherical terminus of the inner FAIMS electrode, the results shown in Fig. 8 are unambiguous. If the cloud did not exist, there could be no high intensity pulse of ions extracted after an ion storage period.

5.4. Ion storage time

An experiment was performed to determine the effect of the length of the ion storage period on the

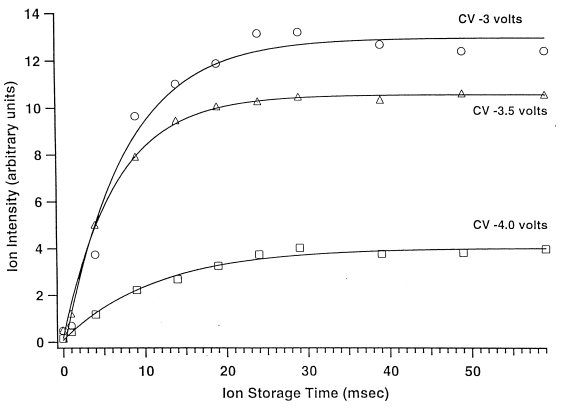

Fig. 9. Intensity of the pulse of ions (*m/z* 380) extracted from the FAIMS ion trap after ion trapping periods of duration up to 60 ms. The solid traces are least squares fits to the data based on a simple kinetic model of the trapping, $Z(t) = (X/k)(1 - e^{-kt})$.

intensity of the pulse of ions extracted from the trapping zone near the end of the inner FAIMS electrode. The intensity of the TOFMS peak for the ion at *m/z* 380 is plotted as a function of the storage period in Fig. 9, at CV = −3, −3.5, and −4 V. The pulses applied to the sampler cone consisted of a variable period at high voltage (OR = +40 V) during which ions were trapped in FAIMS, and a constant time (10 ms) at low voltage (OR = +1 V) to extract ions from FAIMS. The ion storage time appears on the *x* axis of Fig. 9. The signal intensity for the *m/z* 380 ion was measured by pulsing the TOFMS acceleration grids 4.5 ms after OR was lowered. At each of the CVs shown in Fig. 9, the ion intensity rises for over 30 ms. At times in excess of 30 ms, the trap has reached a steady state, wherein the influx of ions via the gas flow is balanced by ion losses through diffusion, ion-ion repulsion and gas flows.

The trapping experiment can be considered to be a kinetics problem. The influx of ions is *X* ions/s. The loss of ions, *Y* ions/s, is proportional to the number of ions in the trap. The increase in the number of ions in the trap, *Z* ions total, will continue until steady state is reached and $X = Y = kZ$, where *k* is the rate constant for the function describing the rate of ion loss from the trap. At a short delay time, *Z* is small and *kZ* is small. It therefore can be assumed that $Z = Xt$ where *t* is the time. The solution to the differential

equation $dZ/dt = X - kZ$ is $Z(t) = (X/k)(1 - e^{-kt} + Z_0 e^{-kt}$, where Z_0 is the ion intensity present in the trap at $t = 0$. The solid curves in Fig. 9 are based on the values of X and k, which were determined from a fit to the data points. The k values were 0.13, 0.15, and 0.09 ms^{-1} for the CV curves −3, −3.5, and −4 V, respectively. The lifetimes (half-life) of the ions in the trap are therefore about 5 ms near CV −3.5 V and about 8 ms at CV −4 V. The corresponding X values were 1.7, 1.6, and 0.35 (intensity/ms), respectively.

The two most important indicators of the three dimensional trapping of ions in the FAIMS ion trap have been demonstrated: first, the existence of a pulse of ions detected via extraction from the trap, and second, a predictable variation in pulse intensity of extracted ions as a function of ion storage time.

Acknowledgement

The authors thank the Mine Safety Appliances Company, Pittsburgh, PA for support in this project.

References

[1] W. Paul, H. Steinwedel, German patent no. 944 900 (1956), US patent no. 2 939 952 (1960).
[2] Royal Swedish Academy of Sciences, Press Release, 12 October 1989, p. 5.
[3] W. Paul, Rev. Mod. Phys. 62 (1990) 531.
[4] H.G. Dehmelt, Rev. Mod. Phys. 62 (1990) 525.
[5] F.A. Londry, G.J. Wells, R.E. March, Hyper. Interac. 81 (1993) 179.
[6] R.E. Kaiser, R.G. Cooks, G.C. Stafford, J.E.P. Syka, P.M. Hemberger, Int. J. Mass Spectrom. Ion Processes 106 (1991) 79.
[7] B.D. Nourse, K.A. Cox, R.G. Cooks, Org. Mass Spectrom. 27 (1992) 453.
[8] P.H. Dawson, Quadrupole Mass Spectrometry and Its Applications, Elsevier, Amsterdam, 1979.
[9] R.E. March, R.J. Hughes, Quadrupole Storage Mass Spectrometry, Wiley-Interscience, New York, 1989.
[10] G. Eiceman, Z. Karpas, Ion Mobility Spectrometry, CRC, Boca Raton, FL, 1994.
[11] Plasma Chromatography, T.W. Carr (Ed.), Plenum, New York, 1984.
[12] E.A. Mason, E.W. McDaniel, Transport Properties of Ions in Gases, Wiley, New York, 1988.
[13] D.I. Carroll, I. Dzidic, E.C. Horning, R.N. Stillwell, Appl. Spectrom. Rev. 17 (1981) 337.
[14] M. Dole, L.L. Mack, R.L. Hines, R.C. Mobley, L.D. Ferguson, M.B. Alice, J. Chem. Phys. 49 (1968) 2240.
[15] J.V. Iribarne, B.A. Thomson, J. Chem. Phys. 64 (1976) 2287.
[16] M. Yamashita, J.B. Fenn, J. Phys. Chem. 88 (1984) 4451.
[17] R.D. Smith, J.A. Loo, R.R. Ogorzalek Loo, M. Busman, H.R. Udseth, Mass Spectrom. Rev. 10 (1991) 359.
[18] I. Buryakov, E. Krylov, E. Nazarov, U. Rasulev, Int. J. Mass Spectrom. Ion Processes 128 (1993) 143.
[19] R.W. Purves, R. Guevremont, S. Day, C.W. Pipich, M.S. Matyjaszczyk, Rev. Sci. Instrum. 69 (1998) 4094.
[20] R. Guevremont, R.W. Purves, Rev. Sci. Instrum. 70 (1999) 1370.
[21] B. Carnahan, A. Tarassov, U.S. patent number 5420424 1995.
[22] R.W. Purves, R. Guevremont, Anal. Chem. 13 (1999) 2346.
[23] D.A. Barnett, B. Ells, R.W. Purves, R. Guevremont, J. Am. Soc. Mass Spectrom, in press.
[24] M.B. Abbot, D.R. Basco, Computational Fluid Dynamics, An Introduction for Engineers, Longman Group, London, UK, 1989, Chap. 8.
[25] R. Guevremont, R.W. Purves, L. Ding, unpublished.